AL-ZAHRAA UNIVERSITY JOURNAL
Health and Medical Science

*Al-Zahraa Journal for Health and Medical Sciences 2026; 4(1):*196-214 **Vol. 4, No.1, 2026**
www.zjhms.alzahraa.edu.iq

Topological analysis of electron density for M-M Metal Bond Clusters (Fe, Ru)

Afraa Naji Tami[1,2]*, Manal Abed Mohammed[1, a], Sajid Hassan Guzar[1, b]

[1] Chemistry Department, College of Science, University of Kerbala, Karbala, 56001, Iraq
[2]Al-Zahraa Centre for Medical and Pharmaceutical Research Sciences (ZCMPRS), Al-Zahraa University for Women, Karbala, 56001, Iraq
* afraa.n@s.uokerbala.edu.iq

Received: 17 March (2026), Accepted: 27 March 2026. Published: 31 March 2026

ABSTRACT

The electron density and multicentre bonding in hexanuclear metal carbide carbonyl clusters is a subject of great controversy within the organometallic community. Closed shell highly reduced metals rarely obey the two-centre rule and so required a more sophisticated description. This paper details a real space description of the bonding in the two extremely stable clusters $Fe_6C(CO)_{17}^{-3}$ and $Ru_6C(CO)_{17}^{-3}$, which consist of a hexa-metal centre surrounded by a central carbide and stabilized by a very tight compact shell of carbonyls. These compounds, bearing a charge of −3, show extreme stability despite great distances between the charges in the clusters. Beyond their fundamental importance in understanding multicentre metal bonding, hexanuclear metal carbide carbonyl clusters may provide valuable insights for the development of metal-based therapeutic agents. In particular, ruthenium carbonyl systems have attracted attention due to their potential biological activity and their relevance in the design of carbon monoxide releasing molecules (CORMs), which are being explored for anti-inflammatory and cytoprotective applications. These electronic differences suggest distinct biomedical potentials. The localized electronic structure of the Fe_6 cluster may favor its use in stable drug delivery systems, while the higher electron delocalization in the Ru_6 cluster may enhance interactions with biological targets, supporting potential applications as anticancer and antimicrobial agents. Additionally, the presence of carbonyl ligands indicates their possible use as CO-releasing molecules (CORMs) with anti-inflammatory activity.

Keywords: Source Function (SF), Delocalization Index, Metal–metal interactions, Electron density topology, highly reduced metal clusters.

AL ZAHRAA UNIVERSITY JOURNAL
Health and Medical Science

*Al-Zahraa Journal for Health and Medical Sciences 2026; 4(1):*196-214 Vol. 4, No.1, 2026
www.zjhms.alzahraa.edu.iq

1. INTRODUCTION

Organometallic transition-metal carbonyl clusters are a class of compounds in which a large number of metal atoms are linked by a variety of metal–metal and metal–ligand bonds. Such compounds are of considerable current interest because their electronic structures are not adequately described by the two-centre model of bonding which is so highly successful in describing the structures and properties of so many organometallic compounds [1,2]. Because of the presence of large numbers of closely spaced metal atoms and strong metal–ligand bonding in many transition-metal carbonyl clusters, highly delocalized electronic structures and multicentre bonding are commonly encountered. An understanding of the bonding in transition-metal clusters is important not only for fundamental reasons but also to account for the unique properties of catalysts, materials, and bioinorganic compounds [3]. Several of the metal carbide complexes and their derivatives mentioned above are members of a large class of unusual organometallic compounds known as the hexanuclear carbide carbonyl clusters. These interesting structures contain six transition metal atoms arranged as a compact three-dimensional structure centred by a μ_6-carbide atom [4]. The clusters are held together by numerous carbonyl bonds which occupy all of the available transition metal coordination sites. The large number of electron pairs on the periphery of the molecule together with the short metal to metal distances lead to considerable ambiguity as to the location of the actual localized bonds between adjacent metal atoms [5]. The highly reduced clusters $Fe_6C(CO)_{17}^{-3}$ and $Ru_6C(CO)_{17}^{-3}$ constitute an important class of compounds in organometallic chemistry. Although highly charged (thrice negative) and electron rich, these complexes are highly stable. So far, experimental and theoretical investigations have dealt mostly with structural aspects and reactivity of these clusters. Less is known about the primary causes of their unusual stability and the nature of the intermetallic bonding in such complexes. It remains a matter of discussion in the literature whether the main contribution to the stability of the clusters is due to the formation of more classical, localized M-M bonds or to more delocalized multicentre bonding distributed across the M—L—M fragments. With the progress of experimental techniques, modern real-space electronic structure analysis has made it feasible to tackle a great number of questions in materials science. The study of the electronic structure via the Quantum Theory of Atoms in Molecules (QTAIM) [1-6] allows to analyse the bonding between atoms by the analysis of the

AL ZAHRAA UNIVERSITY JOURNAL
Health and Medical Science

*Al-Zahraa Journal for Health and Medical Sciences 2026; 4(1):*196-214 Vol. 4, No.1, 2026
www.zjhms.alzahraa.edu.iq

electron density that leads to the topological analysis and thus to understand the electronic behaviour in a molecule, atom or crystal. Complementary descriptors like the Electron Localization Function (ELF), the Source Function (SF) and the delocalization index δ(A,B) give a complete image of the electron density distribution and of the atom involvement on the bonding density as well as the electron sharing between atomic pairs and thus the complete analysis of the atomic interactions at the molecular scale [7]. These approaches are largely applicable in many cases where conventional concepts such as bond and orbit fail. The electronic structure of highly reduced $Fe_6C(CO)_{17}^{-3}$ and $Ru_6C(CO)_{17}^{-3}$ was investigated by the quantum theory of atoms in molecules. source function and delocalization index methodologies and density functional theory Density functional theory studies within the QTAIM, ELF, SF and DI frameworks have been performed to investigate in detail in real space the electronic structure of the highly reduced forms of the hexanuclear carbonyl clusters $Fe_6C(CO)_{17}^{-3}$ and $Ru_6C(CO)_{17}^{-3}$ to achieve an understanding of their intermetallic bonds within the M_6 cluster framework [8]. Comparison of iron and ruthenium results, made possible here for the first time by performing them at an equal level of theory, is an important objective of this work to obtain insights on the character of the M-M intermetallic bonding which might allow us to explain the unusual high stability of the M_6 fragments in these hexanuclear clusters in terms of either localized three centre metal–metal bonds or cooperative delocalization involving several metallic centres [6,7]. The aim of this study is to investigate the electronic structure and bonding characteristics of the hexanuclear metal carbide carbonyl clusters $[Fe_6C(CO)_{17}]^{-3}$ and $[Ru_6C(CO)_{17}]^{-3}$ using real-space electron density analysis methods. Particular emphasis is placed on the application of QTAIM, ELF, and related topological descriptors to characterize the nature of metal–ligand and intermetallic interactions within the metal core. Through this analysis, the study seeks to clarify the role of electron delocalization and multicenter bonding in stabilizing highly reduced transition metal clusters.

2. EXPERIMENTAL SECTION

2.1 Computational Method

The electronic structure of the hexanuclear carbide carbonyl clusters $Fe_6C(CO)_{17}^{-3}$ and $Ru_6C(CO)_{17}^{-3}$ was investigated by means of density functional theory (DFT) [8,9]. Experimental crystal structures were used as the initial geometries for the clusters and as the starting points for quantum chemical calculations to maintain a direct relationship with the experimentally derived

IRAQI Academic Scientific Journals

AL ZAHRAA UNIVERSITY JOURNAL
Health and Medical Science

*Al-Zahraa Journal for Health and Medical Sciences 2026; 4(1):*196-214 Vol. 4, No.1, 2026
www.zjhms.alzahraa.edu.iq

structural parameters. All calculations were performed using the Gaussian 16 software package. The structures were optimized by using the long-range corrected hybrid exchange–correlation functional ωB97X-D [10,11]. This functional was used because it provides a good balance between exchange and correlation, particularly for large systems with delocalized electrons and strong dispersive interactions. Transition metal carbonyl clusters consist of structures that have σ-donation from CO and π-back donation into the metal d-orbitals, thus the exchange–correlation part needs to treat the delocalization and dispersive interactions between different parts of the molecule accurately [12]. The dispersion corrections given in ωB97X-D also enhances the reliability of structures of carbonyl rich complexes, as non-covalent interactions could be crucial in the description of the structure of the molecule. The LanL2DZ [13] effective core potential (ECP) and associated basis set were used for Fe and Ru atoms to account for relativistic core effects efficiently and economically. The Stuttgart–Dresden (SDD) [14,15] basis set was used for carbon and oxygen atoms since the LanL2DZ does not apply to ligand-cantered effects in the carbonyl complexes as effectively as the SDD basis set. The mixed-basis approach is a good compromise between computational speed and accuracy, especially when heavy transition metals are involved [16]. In each case, optimization without imposition of symmetry was performed to allow the electronic structure of the system to dictate that its ground state is the most stable structure for the given atomic arrangement. Subsequent harmonic vibrational frequency calculations were carried out to confirm that the optimized structures were local minima on the energy surface. Evaluation of both the singlet and triplet states in each case yielded no Favor towards either with the energy differences between the states for each system being less than 3 $*10^{-4}$ Eh thus indicating that each corresponds to the ground state [17]. Topological analysis of the electron density was performed within the framework of the Quantum Theory of Atoms in Molecules (QTAIM) using the AIM2000 program. Local topological characteristics including electron density (ρ), Laplacian of electron density ($\nabla^2\rho$) and energy density components at bond critical points were calculated to understand the nature of the metal–ligand bonding. However, due to the highly reduced nature of the metal clusters studied in this work, which can lead to multicentre electron delocalization that may not be fully understood at the local level, real-space analyses were also carried out. Electron Localization Function (ELF) plots can be employed to demonstrate the pairing and localization of electrons in the clusters and at the same time to

IRAQI Academic Scientific Journals

AL ZAHRAA UNIVERSITY JOURNAL
Health and Medical Science

*Al-Zahraa Journal for Health and Medical Sciences 2026; 4(1):*196-214 **Vol. 4, No.1, 2026**
www.zjhms.alzahraa.edu.iq

discriminate between localized two-centre bonds and multicentre delocalized bonds [18]. The electron sharing between two atomic pairs can be quantitatively described by the delocalization index δ(A,B) calculated using the Multiwfn program, regardless of the existence of bond paths. Source Function (SF) analysis has been applied to distinguish the relative atomic contributions to the electron density at critical points, revealing that the bonding density of the metallic framework is derived from localized or delocalized cooperation of the atoms in the cluster. All topological analyses were carried out using wavefunctions derived from the same set of optimized structures [19].

3. RESULTS AND DISCUSSION

3.1 Structural Optimization

Optimization of the geometry of the hexanuclear clusters $Fe_6C(CO)_{17}^{-3}$ and $Ru_6C(CO)_{17}^{-3}$, using the ωB97X-D methodology, in the absence of symmetry constraints, confirms the relevance of the M_6 cage formed by six metal atoms, located around a μ_6 carbide (interstitial atom) and anchored to carbon by means of 17 CO ligand (Fig.1). Therefore, the proposed model accurately describes these reduced clusters. Fe–C bond distances in the iron cluster range from 1.73 Å to 1.87 Å, a value typical for iron carbonyls and due to different local coordination at the metal sites. The C–O bond lengths are as expected for carbonyl coordinated to transition metals providing a proper balance between σ-donation and metal-to-ligand π-back donation. There are small differences in the average Ru–C bond length for the Ru_6 cluster. In particular the larger radial extension and greater spatial diffuseness of the Ru 4d orbitals, as compared with the Fe 3d orbitals, result in a slightly longer metal frame. However, with optimized metal–metal separations corresponding to a compact hexanuclear structure that indicates considerable intermetallic overlap, the question remains whether the metal framework is held together by direct metal–metal bonds. While the structures reveal that the metal–ligand framework and the central carbide function are dominant factors contributing to the overall stability of the clusters, they provide an ideal basis for investigating in detail the real space electron density distribution within the metal frames of the clusters.

IRAQI Academic Scientific Journals

AL ZAHRAA UNIVERSITY JOURNAL
Health and Medical Science

*Al-Zahraa Journal for Health and Medical Sciences 2026; 4(1):*196-214 **Vol. 4, No.1, 2026**
www.zjhms.alzahraa.edu.iq

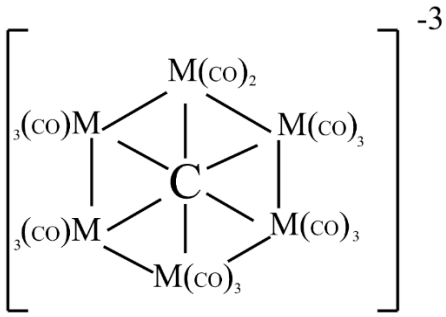

Fig.1. Schematic structure of M= $FeC(CO)_{17}^{-3}$ and $RuC(CO)_{17}^{-3}$ clusters.

3.2 Molecular Graphs and Topological Properties

Electron density topologies for both $Fe_6C(CO)_{17}^{-3}$ and $Ru_6C(CO)_{17}^{-3}$ species have been investigated, using the QTAIM approach and related data that can be extracted from corresponding molecular graphs and electron density topologies [20] (Fig.2). Most of the bond paths together with corresponding bond critical points, in both systems, correspond to M-C and C-O type bonding in the metal-ligand complexes. Several of the M···M contacts within the hexanuclear metal core of 3 do not contain bond critical points (BCP) despite being relatively short [21]. This observation suggests that the mere proximity of the metal centers in these highly reduced species does not signify localized two-center metal–metal bonding. The occurrence of ring critical points (RCPs) within the metal frame suggests a cyclic electron-density topology compatible with multicenter electronic interactions. The molecular graphs of the complexes show clearly separated strongly localized metal—ligand bonding and more delocalized metal core electron systems [4]. We conclude that the M_6 frame of the complexes is stabilized by ligand-mediated multicenter electron delocalization rather than by the formation of classical localized metal—metal bonds [5-9].

IRAQI Academic Scientific Journals

AL ZAHRAA UNIVERSITY JOURNAL
Health and Medical Science

*Al-Zahraa Journal for Health and Medical Sciences 2026; 4(1):*196-214 **Vol. 4, No.1, 2026**
www.zjhms.alzahraa.edu.iq

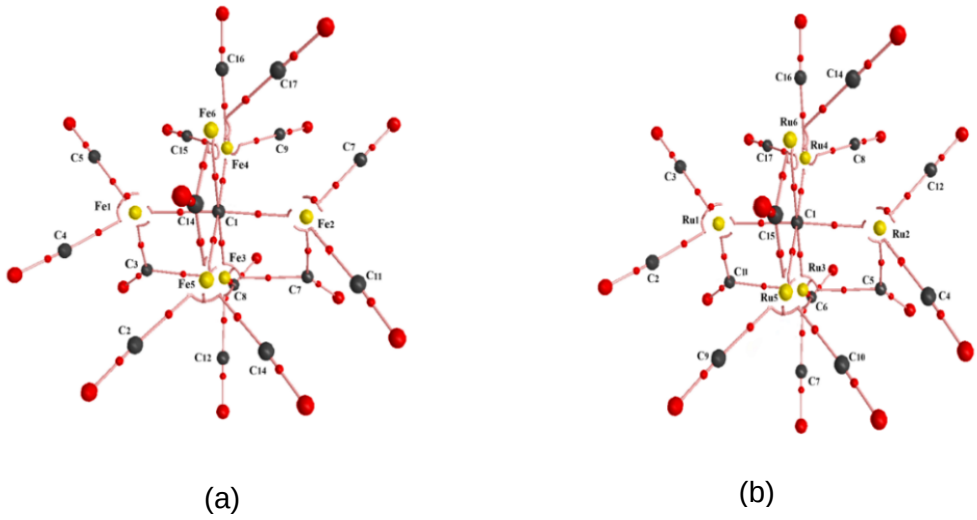

(a) (b)

Fig 2. QTAIM molecular graphs of (a) $Fe(CO)_{17}^{-3}$ and (b) $Ru(CO)_{17}^{-3}$ clusters, showing bond paths (black lines), bond critical points (BCPs, red spheres), and ring critical points (RCPs, yellow spheres).

3.3 Atomic Charge

In an effort to gain more insight into the electronic structure of the $Fe_6C(CO)_{17}^{-3}$ and $Ru_6C(CO)_{17}^{-3}$ clusters, plots of the atomic charge distribution are shown (Table1). In the iron system all iron atoms carry a negative charge from -0.159 e to -0.890 e, indicating that the excess electron density remains relatively confined to the metal framework. The relative broadness of the distribution further supports the non-uniform environment that the iron atoms occupy. In contrast, the ruthenium cluster shows positively charged sites on all Ru atoms (+0.562 to +0.545 e), because the metals can more strongly donate their electrons to the weakly bonded carbonyl ligands, due to their higher radial extension and polarizability of the Ru 4d orbitals. Charge analysis is used to elucidate the electronic differences between the two clusters. The iron cluster retains localized electron density on the metal framework. In contrast, the ruthenium cluster has a more delocalized electronic character, which is facilitated by cooperative metal-ligand interactions.

AL ZAHRAA UNIVERSITY JOURNAL
Health and Medical Science

*Al-Zahraa Journal for Health and Medical Sciences 2026; 4(1):*196-214 Vol. 4, No.1, 2026
www.zjhms.alzahraa.edu.iq

Table 1. Atomic charges (e) of the Fe_6 and Ru_6 clusters.

Atoms	Charge	
	Fe^{-3}	Ru^{-3}
M_1	-0.255	0.562
M_2	-0.159	0.589
M_3	-0.236	0.249
M_4	-0.301	0.624
M_5	-0.890	0.275
M_6	-0.293	0.545

3.4. Local Topological Parameters of M-M Interactions

In the present work, local topological descriptors within the QTAIM approach have been used to elucidate the nature of the metal–metal interactions in the clusters $Fe_6C(CO)_{17}^{-3}$ and $Ru_6C(CO)_{17}^{-3}$. Specifically, it was found that, despite the short intermetallic distances within the hexanuclear structure of the clusters, there are some metal atoms between which no bond critical points (BCPs) are located [18]. As a consequence, local topological descriptors such as electron density (ρ) and Laplacian ($\nabla^2\rho$) of the M–M contact cannot be directly calculated (Table 2). The energy-based descriptors behave in quite different manners for iron and ruthenium clusters. The positive values of the kinetic energy density ratio $G_b/\rho(b)$ (he^{-1}) and the total energy density ratio $H_b/\rho(b)$ (he^{-1}) for all types of interactions point to the coordinative, closed-shell character of the interaction pairs. The potential energy density V_b (he^{-1}) in the nucleus is higher for ruthenium than for iron both for atomic and for cluster interactions. The electron density at the bonding center is higher in Ru–C and Ru–CO bonds, suggesting a stronger attraction in the ruthenium system. Moreover, the ellipticity ε(b). In some cases, higher ε(b) values are obtained for Ru bonds accompanied by higher π-character and thus higher electron delocalization. Iron clusters generally have smaller ellipticity values, indicating a more symmetric σ-bonding situation. Ruthenium has stronger and more delocalized bonds than iron, and this is consistent with the greater extension of the 4d orbitals of ruthenium. This means that localized two-center metal–metal bonding is not the main effect governing the M–M interactions in the two clusters. Topological characteristics are more pronounced in the iron cluster. The iron cluster has no Fe-

IRAQI Academic Scientific Journals

AL ZAHRAA UNIVERSITY JOURNAL
Health and Medical Science

*Al-Zahraa Journal for Health and Medical Sciences 2026; 4(1):*196-214 **Vol. 4, No.1, 2026**
www.zjhms.alzahraa.edu.iq

Fe BCPs which agrees with very small delocalization indices for most of the Fe-Fe pairs [10]. The ruthenium cluster has somewhat larger Ru-Ru electron sharing but again the corresponding topological features of the electron density are diffuse and without any well-defined BCPs [11-22]. It seems that the electronic communication between the metal cores in these molecules cannot be adequately explained by a local bonding description. Instead, the stabilization of the M_6 geometry observed for these species must be attributed to a multicenter delocalization of the valence electrons mediated by the metal-carbonyl framework rather than to discrete localized metal–metal bonds [8-12] show in (Fig. 3,4).

Table 2. The topological properties at the bond critical point of clusters 1-2.

Bond	$\rho(b)$ (eÅ^{-3})		$\nabla^2\rho(b)$ (eÅ^{-5})		$G_b/\rho(b)$ (he^{-1})		$H_b/\rho(b)$ (he^{-1})		V_b (he^{-1})		$\varepsilon(b)$	
	Fe	Ru	Fe	Ru	Fe	Ru	Fe	Ru	Fe	Ru	Fe	Ru
M_1-C_3	0.123	0.122	0.556	0.280	0.189	0.114	0.050	0.043	0.239	0.157	5.518	2.279
M_1-C_1	0.106	0.160	0.256	0.612	0.097	0.216	0.032	0.063	0.130	0.280	5.066	1.033
M_1-C_4	0.106	0.162	0.340	0.604	0.120	0.217	0.034	0.065	0.155	0.283	8.703	9.611
M_1-C_5	0.103	0.120	0.472	0.256	0.151	0.111	0.034	0.046	0.185	0.158	1.943	6.979
M_2-C_1	0.104	0.164	0.264	0.612	0.099	0.220	0.032	0.066	0.133	0.287	2.253	1.296
M_2-C_6	0.105	0.137	0.484	0.304	0.156	0.130	0.035	0.053	0.191	0.183	4.174	1.466
M_2-C_7	0.133	0.112	0.268	0.248	0.126	0.104	0.059	0.041	0.186	0.145	2.747	6.816
M_2-C_{12}	0.103	0.163	0.448	0.612	0.144	0.220	0.031	0.066	0.175	0.286	1.823	9.597
M_3-C_1	0.093	0.098	0.276	0.220	0.092	0.086	0.023	0.030	0.116	0.117	2.567	1.403
M_3-C_7	0.339	0.427	0.304	0.360	0.421	0.793	0.498	0.703	0.919	0.496	5.895	5.355
M_3-C_8	0.102	0.161	0.464	0.612	0.148	0.217	0.032	0.063	0.181	0.281	1.560	2.156
M_3-C_{13}	0.454	0.111	0.812	0.232	0.957	0.099	0.754	0.041	0.711	0.140	2.050	1.638
M_4-C_1	0.065	0.141	0.148	0.364	0.049	0.147	0.011	0.055	0.060	0.202	2.168	3.312
M_4-C_9	0.104	0.162	0.352	0.596	0.122	0.216	0.033	0.066	0.156	0.282	2.432	3.367
M_4-C_{10}	0.106	0.114	0.368	0.252	0.126	0.106	0.034	0.043	0.161	0.150	1.441	4.760
M_4-C_{14}	0.118	0.162	0.332	0.600	0.130	0.215	0.046	0.065	0.177	0.280	9.599	7.466
M_5-C_{11}	0.107	0.119	0.420	0.284	0.142	0.109	0.037	0.037	0.179	0.147	7.990	1.005
M_5-C_{12}	0.124	0.171	0.324	0.640	0.135	0.234	0.054	0.073	0.190	0.307	1.608	9.427

IRAQI Academic Scientific Journals

AL ZAHRAA UNIVERSITY JOURNAL
Health and Medical Science

*Al-Zahraa Journal for Health and Medical Sciences 2026; 4(1):*196-214 **Vol. 4, No.1, 2026**
www.zjhms.alzahraa.edu.iq

M_5-C_1	0.071	0.114	0.232	0.244	0.070	0.104	0.012	0.043	0.083	0.147	1.861	2.567
M_5-C_{15}	0.124	0.100	0.324	0.244	0.135	0.092	0.054	0.030	0.190	0.123	4.864	9.742
M_6-C_1	0.101	0.120	0.272	0.256	0.098	0.112	0.029	0.047	0.128	0.159	1.062	7.442
M_6-C_{15}	0.102	0.122	0.432	0.280	0.140	0.114	0.031	0.043	0.172	0.157	4.439	6.887
M_6-C_{16}	0.150	0.273	0.288	0.300	0.150	0.617	0.077	0.872	0.228	0.490	1.938	9.993
M_6-C_{17}	0.097	0.162	0.464	0.404	0.146	0.217	0.028	0.066	0.175	0.283	1.424	4.701
C-O*	0.454	0.421	0.188	0.167	0.947	0.755	0.758	0.688	0.706	1.444	2.477	1.977

*Average

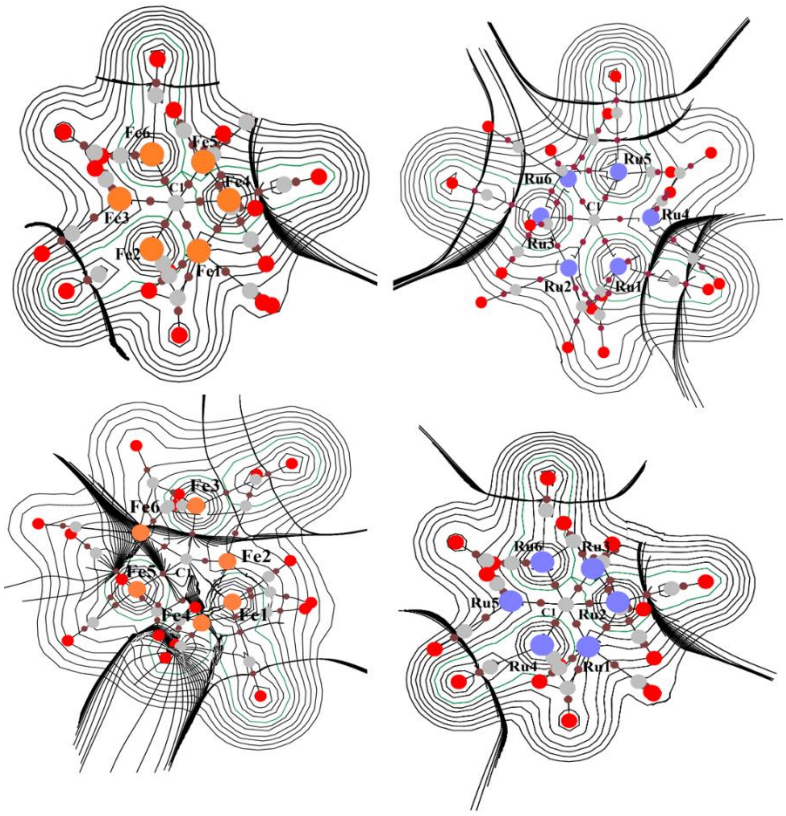

Fig.3. Gradient trajectories mapped on the total electron density for $[FeC(CO)_{17}]^{-3}$ and $[RuC(CO)_{17}]^{-3}$ clusters, illustrating atomic basins, bond paths, and critical points in selected planes of the clusters.

AL ZAHRAA UNIVERSITY JOURNAL
Health and Medical Science

*Al-Zahraa Journal for Health and Medical Sciences 2026; 4(1):*196-214 Vol. 4, No.1, 2026
www.zjhms.alzahraa.edu.iq

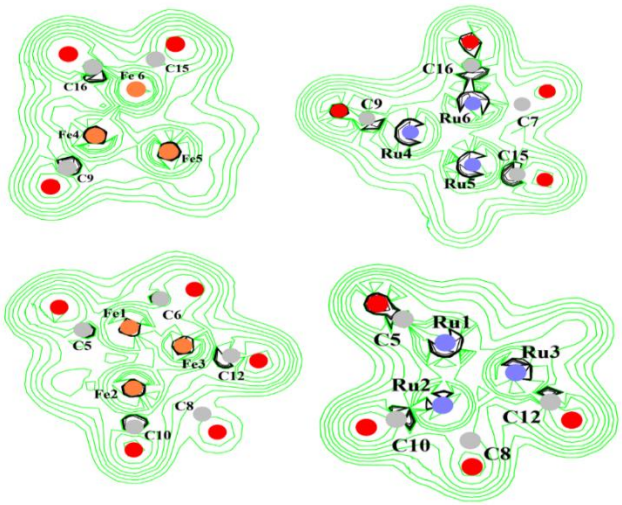

(1) (2)

Fig.4. Laplacian of the electron density for the $[FeC(CO)_{17}]^{-3}$ and $[RuC(CO)_{17}]^{-3}$ clusters in selected planes. Regions of charge concentration (negative $\nabla^2\rho$) and charge depletion (positive $\nabla^2\rho$) illustrate the absence of localized two-center metal–metal bonding.

3.5 Delocalization Indices (DI) Analysis

To gain more insight into the electronic communication within the metal frames of the species under investigation, the delocalization indices δ(A,B) are calculated to measure the electron sharing between pairs of atoms in an oblivious fashion towards the bond paths [23] (Table 3). The delocalization indices for Fe–Fe interactions in $[Fe_6C(CO)_{17}]^{-3}$ were found to be very small (δ ≈ 0.002–0.019) confirming the low degree of electron sharing between the metal atoms as inferred from the almost null values of the delocalization indices and consequently confirming the absence of localized Fe–Fe bonding that was inferred from the QTAIM treatment. In contrast to that, the $[Ru_6C(CO)_{17}]^{-3}$ cluster has significantly larger Ru–Ru delocalization indices with values ranging between δ ≈ 0.45 and 0.56. In Despite not always being located on corresponding bond critical points, the values suggest a rather substantial sharing of the electron density between the respective Ru pairs, in conjunction with a more collective and delocalized electron distribution within the ruthenium part of the clusters [19-24]. The M–C* delocalization indices are quite similar for almost all the metal centers, which means that the central carbide in these compounds is involved in MC* multicenter delocalization with the metal framework [25].

IRAQI Academic Scientific Journals

AL ZAHRAA UNIVERSITY JOURNAL
Health and Medical Science

*Al-Zahraa Journal for Health and Medical Sciences 2026; 4(1):*196-214 **Vol. 4, No.1, 2026**
www.zjhms.alzahraa.edu.iq

In addition, the delocalization indices associated to the metal–carbonyl bonding is still relatively high and they reflect the strong metal to ligand electron sharing associated with the π-back-donation [26]. DI analysis on the electron sharing between the metal atoms concludes that the electron sharing cannot be described by localized two-center bonds. Instead, a multicenter delocalization of the electrons through the metal-carbonyl framework is proposed as the main contribution to the metal-metal bonding with a higher degree of intermetallic delocalization being inferred for the Ru_6 cluster than for the Fe_6 cluster [27].

Table 3. Delocalization Indexes for selected atomic δ (A, B) interaction in cluster 1- 2

Atom Pair (A, B)	δ (A, B)		Atom Pair (A, B)	δ (A, B)	
	Fe	Ru		Fe	Ru
M_1-M_2	0.019	0.508	M_4-M_5	0.013	0.390
M_1-M_3	0.008	0.454	M_4-M_6	0.013	0.009
M_1-M_4	0.007	0.545	M_5-M_6	0.004	0.191
M_1-M_5	0.006	0.537	M_1-C*	0.289	0.274
M_1-M_6	0.003	0.251	M_2-C*	0.261	0.252
M_2-M_3	0.004	0.565	M_3-C*	0.274	0.247
M_2-M_4	0.002	0.101	M_4-C*	0.303	0.260
M_2-M_5	0.002	0.410	M_5-C*	0.246	0.243
M_2-M^6	0.009	0.007	M_6-C*	0.022	0.007
M_3-M_4	0.007	0.538	$M_{C\text{-}O^*}$	2.210	2.201
M_3-M_5	0.002	0.110			
M_3-M_6	0.008	0.007			

* Average

3.6 Source Function (SF) Analysis of M-M Interactions

By application of the Source Function (SF) analysis the atomic contributions to the electron density associated with the metal–metal interaction regions were derived [28]. While the Fe atoms involved in Fe–Fe interactions account for about 3.12% of the total electron density at these regions the iron centers not involved contribute less than 0.185%. Likewise, the

IRAQI Academic Scientific Journals

AL ZAHRAA UNIVERSITY JOURNAL
Health and Medical Science

*Al-Zahraa Journal for Health and Medical Sciences 2026; 4(1):*196-214 Vol. 4, No.1, 2026
www.zjhms.alzahraa.edu.iq

contributions of the central carbide and the carbonyl ligands are small (0.52% and 5.09% respectively). This clear-cut partitioning of the electron density in the Fe framework of the $Fe_6C(CO)_{17}^{-3}$ cluster points towards a very low degree of mutual cooperation of the metal atoms in space, which is fully supported by the very small delocalization indices of the Fe–Fe bonds in the cluster and the fact that neither of the Fe–Fe bonds possess a bond critical point. In contrast, the $Ru_6C(CO)_{17}^{-3}$ cluster exhibits very different behavior (Table 4). The contributions due to the bonded Ru-atoms to about 34.43%, while that of the non-bonded Ru-atoms is 13.65%. The contributions due to the carbide and to the carbon-monoxide ligands are very small (−0.06% and −0.09% respectively). This points to a high degree of intra-metallic "co-operation" in the distribution of electron density associated with the Ru–Ru bonding. In contrast, the SF results clearly differentiate the electronic behavior of the two clusters: The Fe 6 cluster has only very small and localized M→L contributions, while the Ru 6 cluster has a highly cooperative electronic behavior involving a large number of Ru atoms. This is in line with the larger Ru–Ru delocalization indices and the increased multicenter electron delocalization of the Ru 6 cluster [29-30] (Table 5).

Table 4. SF contribution (%) of selected atoms to electron density in Fe-Fe BCPs in cluster 1.

Atom	Fe(bond)	Fe(non-bond)	C*	O*
SF%	3.12	0.185	0.52	5.09

* Average

Table 5. SF contribution (%) of selected atoms to electron density in Ru-Ru BCPs in cluster 2.

Atom	Ru(bond)	Ru(non-bond)	C*	O*
SF%	34.43	13.65	-0.06	-0.09

* Average

3.7 Electron Localization Function (ELF) Analysis

To examine possible differences in the ELDs of the $Fe_6C(CO)_{17}^{-3}$ and $Ru_6C(CO)_{17}^{-3}$ clusters and to better understand the electronic structures of their metal frameworks, the ELF distributions are compared in the two clusters. Similar distributions are seen for high ELF values around the O atoms and along the C—O bonds in the CO ligands, indicative of the lone pairs on the oxygen atoms and the multi-bonding within these ligands [31]. Similarly, the same type of ELF basin is seen along the M-C bonds. The differences within the metal cores are, however,

IRAQI Academic Scientific Journals

AL ZAHRAA UNIVERSITY JOURNAL
Health and Medical Science

*Al-Zahraa Journal for Health and Medical Sciences 2026; 4(1):*196-214 **Vol. 4, No.1, 2026**
www.zjhms.alzahraa.edu.iq

pronounced. In the Fe_6 cluster the ELF in the Fe···Fe region is very low between any pair of iron atoms. Thus, there is no significant evidence of localized electron pairing between neighboring iron atoms, and the electron density is maintained within the metal–ligand framework. This is also in full agreement with the QTAIM model that shows no Fe–Fe BCPs and very small Fe–Fe delocalization indices [25-31] (Fig 5). In contrast to the iron species the ELF associated with the Ru_6 cluster extends over a larger area encompassing most of the Ru nuclei. Even though there is no indication of the formation of clearly separated localized Ru–Ru bonding basins the area occupied by the ELF in between the Ru nuclei is larger and more diffuse, which is consistent with a more cooperative and therefore intermetallic character of the electron density, thus indicating a better interaction between the metal centers in the ruthenium cluster when compared with the iron. The comparison reveals a clear electronic difference between the two clusters [12-22] (Fig 6). The iron cluster is characteristic of localized bonding between the transition metal center and the ligands and exhibits very little transfer of electrons between the metal centers. In contrast, the ruthenium cluster indicates a more delocalized electronic picture, with higher multicenter bonding between the metal centers, indicating more extensive delocalization of the electron density [14]. These differences are attributable to the larger radial extent and larger polarizability of Ru 4d orbitals compared to the Fe 3d orbitals, confirming that the type of bonding found in the transition metal cores of the clusters is based on cooperative multicenter bonding rather than localized metal—metal bonding [9].

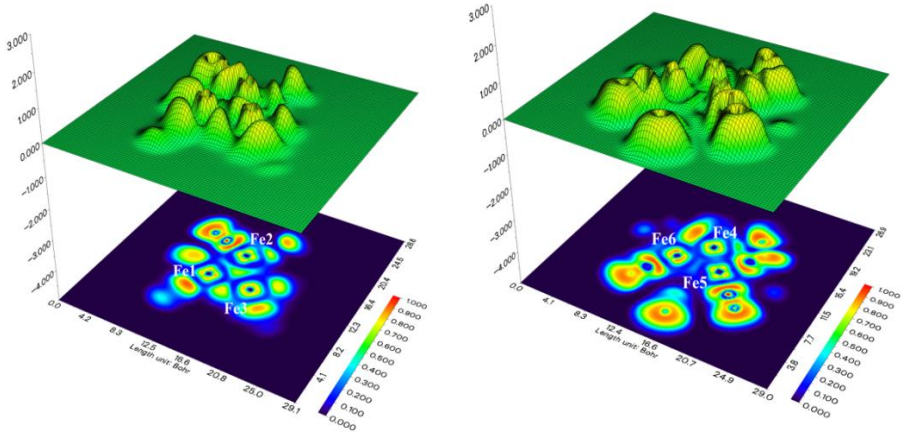

Fig 5. Two-dimensional ELF projections for the $FeC(CO)_{17}^{-3}$ cluster in selected planes, highlighting localized electron density associated with carbonyl ligands and the central carbide carbon, and delocalized regions within the metal framework.

IRAQI Academic Scientific Journals

AL ZAHRAA UNIVERSITY JOURNAL
Health and Medical Science

*Al-Zahraa Journal for Health and Medical Sciences 2026; 4(1):*196-214 **Vol. 4, No.1, 2026**
www.zjhms.alzahraa.edu.iq

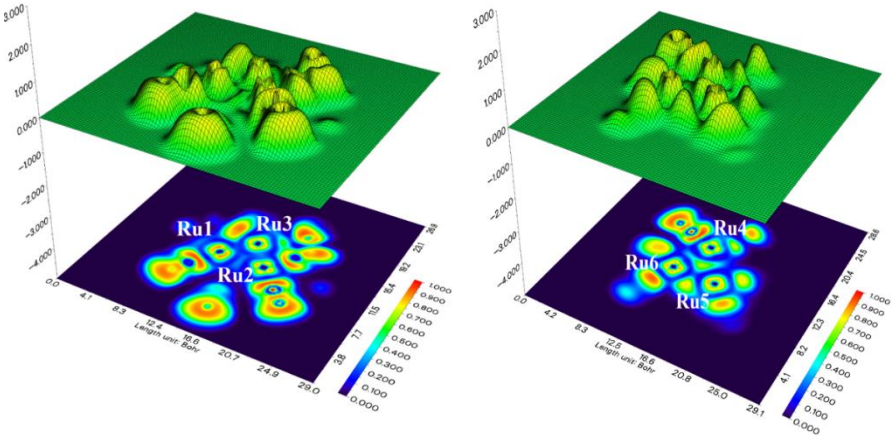

Fig 6. Two-dimensional ELF projections for the $RuC(CO)_{17}^{-3}$ cluster in selected planes, showing ligand-centered electron localization and enhanced delocalization over the Ru_6 metal cage.

Conclusion

Investigate the possibility of differences between the ELDs of the $Fe_6C(CO)_{17}^{-3}$ and $Ru_6C(CO)_{17}^{-3}$ clusters and gain insight into the metallic part of the electronic structure of these complexes by comparing the ELF distribution in the two systems. The high ELF values in the vicinity of the O atoms and along the C—O bonds in the CO ligands are indicative of the lone pairs associated with the oxygen atoms, as well as the multi-bonding character in the CO ligands, and the same type of ELF basin is observed along the M—C bonds. There is no appreciable difference between the overall shapes of the electron localization functions (ELF) for the different clusters, apart from differences within the metal cores. Thus, in the Fe_6 cluster the ELF is very low between any pair of Fe atoms in the Fe···Fe region; there is therefore no indication of localized electron pairing between adjacent iron atoms and the electron density is confined within the metal–ligand framework. This is also in agreement with the QTAIM model, which affirms that there is no Fe–Fe bond critical points (BCPs) and the Fe–Fe delocalization indices are very small. In contrast to the iron species the ELF associated with the Ru_6 cluster spans a larger area including most of the Ru nuclei. Although there is no evidence of well-defined localized Ru–Ru bonding basins the area occupied by the ELF in between the Ru nuclei is larger and more diffuse, which is indicative of a more cooperative and therefore intermetallic character of the electron density between the metal centers in the ruthenium cluster, pointing therefore to a stronger

IRAQI Academic Scientific Journals

AL ZAHRAA UNIVERSITY JOURNAL
Health and Medical Science

*Al-Zahraa Journal for Health and Medical Sciences 2026; 4(1):*196-214 **Vol. 4, No.1, 2026**
www.zjhms.alzahraa.edu.iq

interaction between the metal centers in the ruthenium cluster than in the iron. Comparison of iron and ruthenium clusters with similar structures shows a clear electronic difference.

The ELF and QTAIM analyses reveal clear electronic differences between the Fe_6 and Ru_6 clusters despite their similar structural frameworks. In the Fe_6 cluster, the electron density is largely localized within the metal–ligand framework with no evidence of Fe–Fe bonding, consistent with very small delocalization indices. In contrast, the Ru_6 cluster exhibits a more diffuse ELF distribution across the metal core, indicating stronger multicenter interactions due to the polarizable Ru 4d orbitals. Maybe, Studying the electronic structure and bonding characteristics of these clusters may contribute to the rational design of metal-based therapeutics, particularly CO-releasing molecules (CORMs) with anti-inflammatory and anticancer activity, as well as antimicrobial agents and drug delivery systems. In addition, the electronic properties of such clusters may support their application in bioimaging and diagnostic technologies

Acknowledgements

The authors gratefully acknowledge the institutional support of the University of Kerbala and Al-Zahraa University for Women.

Conflict of Interest

Conflict of Interest: The authors declare that they have no conflicts of interest.

Reference

1. Cotton, F.A. (1978) ‘Discovering and understanding multiple metal-to-metal bonds’, Accounts of Chemical Research, 11(6), pp.225–232. https://doi.org/10.1021/ar50126a001
2. Sikkander, A.R.M., Meena, M., Yadav, H., Wahi, N. and Lakshmi, V.V. (2024) ‘Appraisal of the impact of applying organometallic compounds in cancer therapy’, Journal of Applied Organometallic Chemistry, 4(2), pp. 145–166. https://doi.org/10.48309/JAOC.2024.433120.1154
3. Adams, R.D. and Captain, B. (2009) ‘Unusual structures and reactivity of mixed metal cluster complexes containing the palladium/platinum tri-tert-butylphosphine grouping’, Accounts of Chemical Research, 42(3), pp. 409–418. https://doi.org/10.1021/ar800193e
4. Shieh, M. and Miu, C. (2010) ‘Carbonylchromium chalcogenide complexes: synthesis, reactivity and properties’, Journal of the Chinese Chemical Society, 57(4B), pp. 956–966. **https://doi.org/10.1002/jccs.201000133Digital Object Identifier (DOI)**

AL ZAHRAA UNIVERSITY JOURNAL
Health and Medical Science

*Al-Zahraa Journal for Health and Medical Sciences 2026; 4(1):*196-214 **Vol. 4, No.1, 2026**
www.zjhms.alzahraa.edu.iq

5. Frenking, G. and Krapp, A. (2007) 'Unicorns in the world of chemical bonding models', Journal of Computational Chemistry, 28(1), pp.15–24. **https://doi.org/10.1002/jcc.20543Digital Object Identifier (DOI)**
6. Gatti, C. and Lasi, D. (2007) 'Source function description of metal–metal bonding in d-block organometallic compounds', Faraday Discussions, 135, pp.55–78. **https://doi.org/10.1039/B605404H**
7. Bader, R.F.W. and Nguyen-Dang, T.T. (1981) 'Quantum theory of atoms in molecules—Dalton revisited', in Advances in Quantum Chemistry. Elsevier, pp.63–124. https://doi.org/10.1016/S0065-3276(08)60326-3
8. Fianchini, M. and Mikhailov, O.V. (2022) 'Introduction from guest editors to special issue "Multi-metallic systems: from strong cooperative bonds to weak M–M interactions"', International Journal of Molecular Sciences, 23(19), p.10998. https://doi.org/10.3390/ijms231910998
9. Cesari, C., Bortoluzzi, M., Funaioli, T., Femoni, C., Iapalucci, M.C. and Zacchini, S. (2023) 'Highly reduced ruthenium carbide carbonyl clusters: synthesis, molecular structure, reactivity, electrochemistry, and computational investigation of $[Ru_6C(CO)_{15}]^{4-}$', Inorganic Chemistry, 62(36), pp.14590–14603. DOI: 10.1021/acs.inorgchem.3c01711
10. Fuentealba, P., Preuss, H., Stoll, H. and von Szentpály, L. (1982) 'A proper account of core-polarization with pseudopotentials: single valence-electron alkali compounds', Chemical Physics Letters, 89(5), pp.418–422. https://doi.org/10.1016/0009-2614(82)80012-2
11. Sharma, J. and Champagne, P.A. (2022) 'Benchmark of density functional theory methods for the study of organic polysulfides', *Journal of Computational Chemistry*, 43(32), pp.2131–2138. https://doi.org/10.1002/jcc.27007Digital Object Identifier (DOI)
12. König, F.B., Schönbohm, J. and Bayles, D. (2001) 'AIM2000—A program to analyze and visualize atoms in molecules', Journal of Computational Chemistry, 22(5), pp.540–545. DOI:10.1002/1096-987X(20010415)22:5<545::AID-JCC1027>3.0.CO;2-Y
13. Lu, T. and Chen, F. (2012) 'Multiwfn: a multifunctional wave function analyzer', Journal of Computational Chemistry, 33(5), pp. 580–592. **https://doi.org/10.1002/jcc.22885Digital Object Identifier (DOI)**

AL ZAHRAA UNIVERSITY JOURNAL
Health and Medical Science

*Al-Zahraa Journal for Health and Medical Sciences 2026; 4(1):*196-214 **Vol. 4, No.1, 2026**
www.zjhms.alzahraa.edu.iq

14. Cremer, D. and Kraka, E. (1984) 'Chemical bonds without bonding electron density—does the difference electron-density analysis suffice for a description of the chemical bond?', *Angewandte Chemie International Edition*, 23(8), pp.627–628. https://doi.org/10.1002/anie.198406271Digital Object Identifier (DOI)
15. Benavides, M. and Granda, E. (2024) 'Au···H−X (X = N or C) intramolecular interactions in gold(I)-NHC carbene complexes with potential anticancer properties: a quantum mechanical study with two basis sets', ChemistryOpen, 13(10), p. e202400140. https://doi.org/10.1002/open.202400140Digital Object Identifier (DOI)
16. Sirat, S.S., Rosli, M.M., Arshad, S., Al-Ibadi, M.A.M., Hassan, A.H., Yusof, E.N.M. and Shawkataly, O.B. (2025) 'Reactions of $Ru_3(CO)_{12}$ with 1,5-bis(diphenylphosphino)pentane: synthesis, characterization, crystal structure, Hirshfeld surface and QTAIM analysis of $Ru_3(CO)_{10}$(μ-dpppe)', Journal of Molecular Structure, 1321, p. 140158. DOI:10.1016/j.molstruc.2024.140158
17. Khan, R.A., Jaafar, M.H., Hadi, A.D., Alsaeedi, H. and Alsalme, A. (2025) 'Luminescent tetranuclear Ag(I)/Cu(I) cubane clusters: investigating argentophilicity, cuprophilicity, and mixed argento-cuprophilicity', Inorganica Chimica Acta, 578, p. 122517. DOI:10.1016/j.ica.2024.122517
18. Al-Otaibi, J.S., Mary, Y.S., Thomas, R. and Costa, R.A. (2023) 'DFT investigations on the interactions between pyrimidine derivatives and Ag/Au/Cu metal clusters: solvation effects and reactivity analysis', Journal of Cluster Science, 34(6), pp. 2847–2858. DOI:10.1007/s10876-023-02429-4
19. Alhimidi, S.R.H., Al-Ibadi, M.A.M. and Jabbar, M.L. (2024) 'QTAIM analysis of the bonding in anionic group 6 carbonyl selenide clusters: $[Se_2M_3(CO)_{10}]^{2-}$ (M = Cr, Mo, W)', Journal of Molecular Modeling, 30(7), p. 230. DOI: 10.1007/s00894-024-06031-x
20. Popelier, P.L.A. (2000) 'On the full topology of the Laplacian of the electron density', Coordination Chemistry Reviews, 197(1), pp.169–189. DOI:10.1016/S0010-8545(99)00189-7
21. Al-Kirbasee, N.E., Hassan, A.H. and Ahmad, H.A. (2023) 'Quantum theory of atoms-in-molecules (QTAIM): study of the bonding in di-ruthenium di-chloro cluster', Chemical and Environmental Science Archives, 3(4), pp.65–69.

AL ZAHRAA UNIVERSITY JOURNAL
Health and Medical Science

*Al-Zahraa Journal for Health and Medical Sciences 2026; 4(1):*196-214 **Vol. 4, No.1, 2026**
www.zjhms.alzahraa.edu.iq

22. Hamza, N.A. and Al-Ibadi, M.A.M. (2023) 'QTAIM view of Fe···Fe binding within triiron clusters [(μ_3-S)Fe_3(CO)$_9$(μ_3-CO)]', Theoretical Chemistry Accounts, 142(11), p.120. DOI:10.1007/s00214-023-03065-x
23. Gassoumi, B., Dlala, N.A., Echabaane, M., Karayel, A., Özkınalı, S., Castro, M.E., Melendez, F.J., Ghalla, H., Nouar, L. and Madi, F. (2022) 'Stability, spectroscopic, electrochemistry and QTAIM analysis of Cu–$Zn_{n-1}O_n$ clusters for glucose sensing application: a study on theoretical and experimental insights', Heliyon, 8(12). DOI: 10.1016/j.heliyon. 2022.e12387
24. Sellin, M., Seiler, M. and Krossing, I. (2023) 'Coordination versus insertion: on the interaction of 5d-transition metal carbonyl clusters with silver(I)', Chemistry – A European Journal, 29(34). https://doi.org/10.1002/chem.202300908Digital Object Identifier (DOI)
25. Becke, A.D. and Edgecombe, K.E. (1990) 'A simple measure of electron localization in atomic and molecular systems', Journal of Chemical Physics, 92(9), pp.5397–5403. https://doi.org/10.1063/1.458517
26. Gatti, C. (2005) 'Chemical bonding in crystals: new directions', Zeitschrift für Kristallographie, 220(5–6), pp.399–457. DOI:10.1524/zkri.220.5.399.65073
27. Frenking, G. and Shaik, S. (2014) The Chemical Bond: Chemical Bonding across the Periodic Table. Wiley. DOI:10.1002/9783527664658.ch7
28. Macchi, P. (2013) 'Modern charge density studies: the entanglement of experiment and theory', Crystallography Reviews, 19(2),pp. 58–101.
29. Silvi, B. and Savin, A. (1994) 'Classification of chemical bonds based on topological analysis of electron localization functions', Nature, 371(6499), pp.683–686. **DOI:** 10.1038/371683a0
30. Pichierri, F. (2022) 'Theoretical insights into the nature of the bonding between carbon monoxide and iron(II) phthalocyanine: how do QTAIM descriptors change as a function of the Fe–CO distance?', Chemical Physics Letters, 804, p.139901. https://doi.org/10.1016/j.cplett.2022.139901
31. Wijesooriya, S.S. and Pandithavidana, D.R. (2022) 'Investigation and comparison of antioxidant potential of catechins present in green tea: DFT study', Chemistry & Chemical Technology, 16(4), pp.591–599. https://doi.org/10.23939/chcht16.04.591